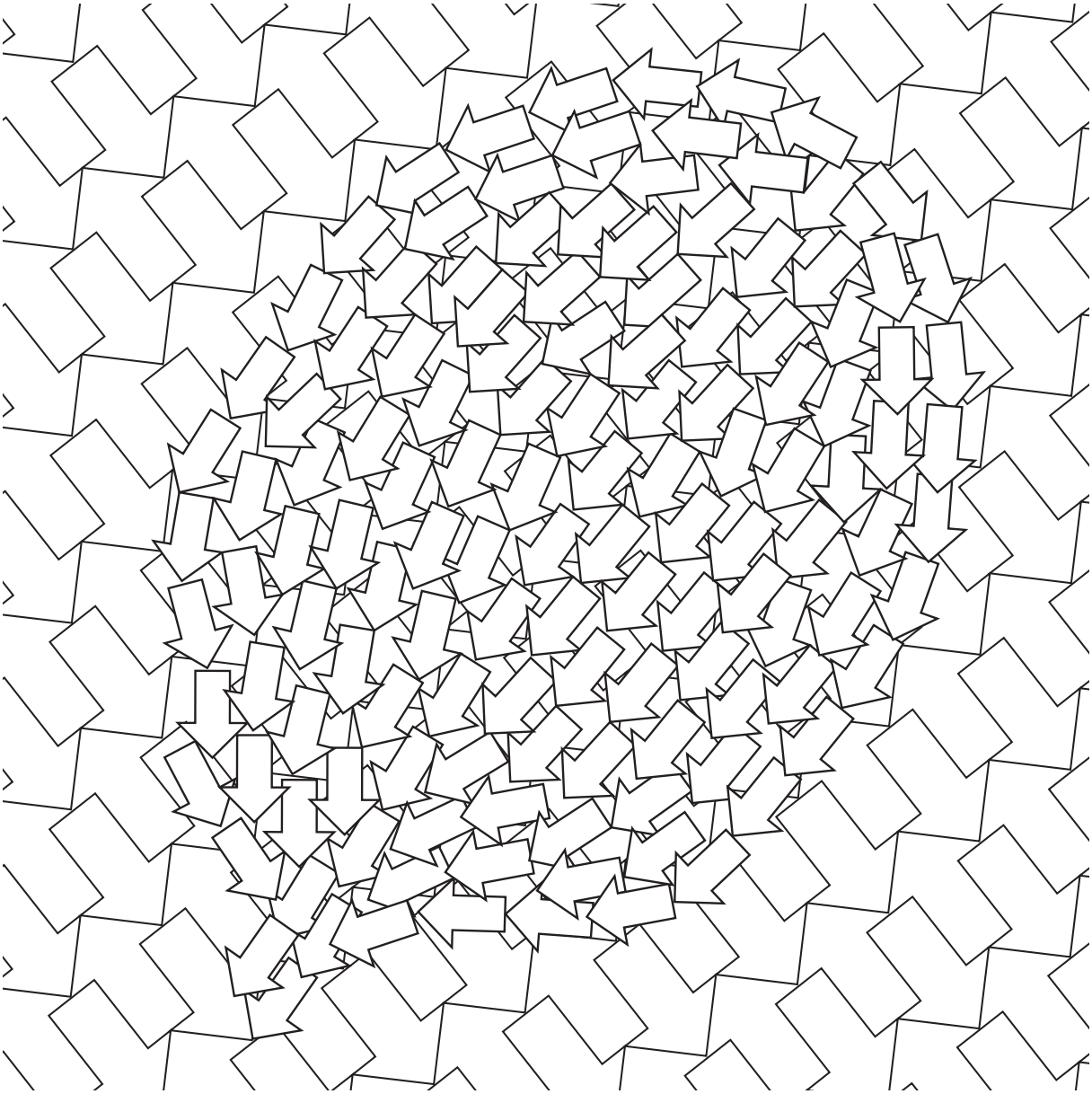

Implication du Syndrome d’économie foliaire dans la résorption de l’azote.

Leaf nitrogen resorption dynamics within the slow-fast continuum in an annual species

Sartori Kevin, Violle Cyrille, Vile Denis, Vasseur François, Pierre de Villemereuil, Bresson Justine, Gillespie Lauren, Fletcher Leila Rose, Sack Lawren, Kazakou Elena

Soumis à *The New Phytologist*

Summary

Few studies have tested the links between leaf nitrogen resorption and whole-plant resource use strategies and performance. Indeed, tests of such potential linkages are hampered by the classical evaluation of plant nitrogen resorption capacity based on 'snapshots' of leaf nitrogen concentration from adult and senescent leaves (the nitrogen resorption efficiency, RE_N).

We greatly increased the resolution for measuring nitrogen resorption by tracking time courses of leaf nitrogen concentration in 121 natural *Arabidopsis thaliana* genotypes native to a wide range of climates across Europe, grown in a greenhouse. In addition to the classical measurement of resorption efficiency measurement, we computed the absolute nitrogen resorption rate (RR_N), i.e., the amount of nitrogen remobilized by a leaf per unit time.

Across genotypes, high rates and efficiency of nitrogen resorption were associated with low leaf photosynthetic capacity ($r = –0.77$, and $r = –0.28$, $P < 0.01$) and long plant lifespan ($r = 0.75$, and $r = 0.23$, $P < 0.01$). The RR_N showed significant heritability, genetic associations, selection, and was negatively correlated across genotypes with the mean annual temperature of the native population. By contrast, RE_N showed low heritability, no evidence of genetic association, and no relationship with climatic variables.

Our results suggest a much stronger adaptive role for leaf nitrogen resorption than previously uncovered.

Introduction

Leaf nitrogen resorption plays a major role in the plant nutrient budget, remobilizing and relocating nitrogen from senescing organs to surviving tissues (Killingbeck, 1986). This process increases nitrogen mean residence time, enabling plants to mitigate the nitrogen limitation that exists in most natural ecosystems (Berendse & Aerts, 1987; Aerts & Chapin, 1999). Despite the tremendous importance of nitrogen resorption for plant physiology and ecology, its contribution to species local adaptation remains unresolved. Nitrogen resorption is indeed a complex, dynamic, and multifaceted molecular choreography barely captured by 'snapshots' of leaf trait measurements (Harper & Sellek, 1987; Reich *et al.*, 1991) as has been the state of the art for comparative ecology (Aerts & Chapin, 1999). In this study, we greatly improved the resolution of nitrogen resorption measurements by recording daily changes in nitrogen concentration and measuring rates of resorption. In addition, we explored the intrinsic and extrinsic drivers of nitrogen resorption within a model species, to improve our understanding of the adaptive nature of this pivotal process.

The search for global patterns in nutrient use strategies in functional ecology has generally focused on variations in leaf lifespan and nutrient concentrations during the "green phase" of the leaf. Leaf lifespan and leaf nutrient concentrations, taken into account alongside specific leaf area (SLA), assimilation, and respiration rates, define a pervasive leaf-level trade-off, the "leaf economics spectrum" (LES) (Wright *et al.*, 2004). The LES describes inter- or intraspecific leaf trait covariations as a slow-fast continuum. On one extreme, species express leaf traits related to rapid metabolism (high photosynthetic rate) over a short lifespan and low investment in structural tissues, and on the other extreme, species express leaf traits related to long-lived leaves with slow metabolism. This leaf-level trade-off may indeed reflect a whole-plant trade-off (Reich, 2014; Salguero-Gómez *et al.*, 2016). Thus, species characterized by "slow" LES traits would grow slowly, reach maturity later, live longer, and more effectively conserve resources over their lifespan (conservative strategy). By contrast, species with "fast" LES traits should grow faster, reach maturity earlier, have shorter lifespans, and more effectively acquire resources (acquisitive strategy). Empirical evidence of the connection between leaf-level and plant-level resource use strategies has been supported by recent intraspecific studies (Sartori *et al.*, 2019). Given that nitrogen mean residence time is a determinant of operational nitrogen concentration (Aerts & Chapin, 1999) one might thus expect that plant resource-use strategies, and thus LES traits would be associated with nitrogen

resorption rate (Kazakou *et al.*, 2007; Freschet *et al.*, 2010). However, the few studies examining the coupling between nitrogen resorption and LES across species did not show consistent patterns (Kazakou *et al.*, 2007; Freschet *et al.*, 2010; Yuan & Chen, 2010; Campanella & Bertiller, 2011; Achat *et al.*, 2018). Higher resolution intraspecific comparisons are needed to control for variation across other traits, and species-specific biochemical and biophysical determinants of nitrogen resorption that may blur the LES traits – resorption efficiency relationship. Moreover, comparing ecotypes within a species can be crucial to understand the role of nitrogen resorption in plant performance and local adaptation given its influence on plant fitness.

Traditional comparative approaches for measuring nitrogen resorption have focused on the proportion of nitrogen resorbed between the adult stage and the end of the leaf life cycle (namely resorption efficiency, RE_N) and the leaf nitrogen concentration at the end of the leaf life cycle (namely nitrogen resorption proficiency) (Aerts & Chapin, 1999). However, there are many ways to obtain comparable nitrogen resorption efficiencies. The dynamics of nitrogen resorption can be informative of the overall metabolic machinery of the leaf and provide a more comprehensive understanding of plants' nutrient-use strategies (Fig. 1). Non-destructive measurements are now possible using near infrared spectroscopy (NIRS) that enables the estimation of material properties from light absorbance (Ecarnot *et al.*, 2013) and can help monitor the temporal variation of leaf nitrogen concentration (Vilmus *et al.*, 2014). We define the absolute nitrogen resorption rate (RR_N) as the amount of nitrogen remobilized by a leaf per unit time. We expect slow-growing plants to exhibit low RR_N over a long leaf lifespan, whereas fast-growing plants should display high RR_N over a short period of time. This is consistent with the expected higher resorption efficiency of slow-growing plants: low rates of resorption over a long period would enable a higher proportion of nitrogen remobilization (Fig. 1).

According to ecology and functional biogeography studies, species or genotypes adapt to harsh environmental conditions with conservative trait values (e.g. Borgy *et al.*, 2017). Thus, we expect higher rates and lower efficiency of resorption for genotypes native to environments that are more favorable. Empirical tests of this assumption remain scarce and limited to local and site-specific studies. Yuan & Chen (2009) performed a meta-analysis, gathering resorption efficiencies across species distributed worldwide. The authors reported a significant decrease in nitrogen resorption efficiency with increasing latitude, temperature, and precipitation. The

comparison of populations of a single species distributed along environmental gradients is now essential to test whether natural selection underlines these patterns.

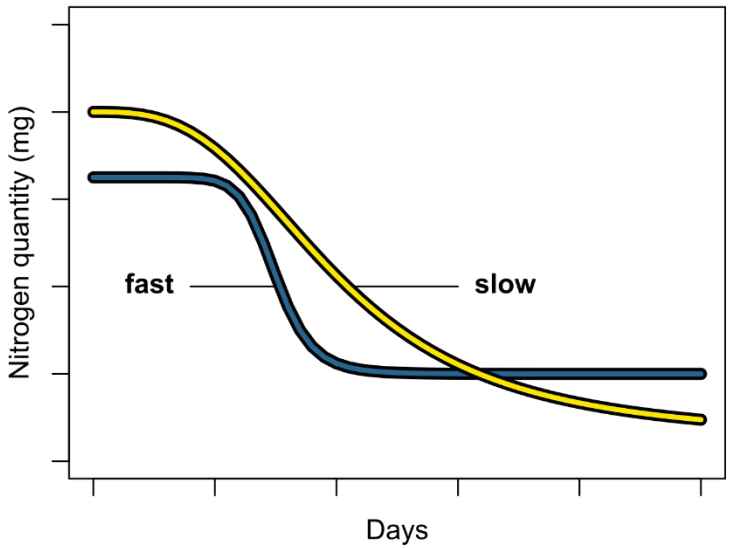

Figure 1: Expected leaf nitrogen dynamics for slow-growing (yellow) versus fast-growing (blue) plants.

Arabidopsis thaliana is a model species for not only genetic studies, but increasingly for ecological studies given its broad climatic range, and large variation in life-history traits (e.g. Mitchell-Olds, 2001; Brachi *et al.*, 2012) and functional traits, notably those related to the LES (Vasseur *et al.*, 2018b; Sartori *et al.*, 2019). *A. thaliana* is an herbaceous annual species with a large distribution spanning from the Mediterranean coast to Northern Sweden and across Asia. This distribution covers considerable variation of climatic conditions that are correlated with the genetic structure of *A. thaliana*'s populations, suggesting underlying local adaptation (Lasky *et al.*, 2012). The genetic determinism of the life cycle length, most often measured as the germination-flowering time interval, has been particularly well explored given its key role in *A. thaliana* adaptation to contrasting environments (e.g., Mendez-Vigo *et al.*, 2011; Lovell *et al.*, 2013; Schmalenbach *et al.*, 2014). Further, recent studies uncovered common genetic bases for flowering time and LES traits (Vasseur *et al.*, 2012), and evidenced that the differentiation of these traits is mediated by abiotic stresses (Vasseur *et al.*, 2018a). Substantial variability in resorption efficiency has been detected among a few genotypes (Masclaux-Daubresse & Chardon, 2011), reflecting variation in the genetic and metabolic pathways

involved in proteolysis and transport of N-bearing molecules (Havé *et al.*, 2017). However, the broader range of natural variability of nitrogen resorption requires assessment for a large panel of genotypes from contrasting environments, including elucidation of its genetic determinants and their importance for local adaptation.

We quantified the phenotypic and environmental variation of nitrogen resorption, and performed a genetic association study using common garden-grown ecotypes representing 121 *A. thaliana* populations sampled across the bulk of their native climate range. We hypothesized (i) strong variability in nitrogen resorption across ecotypes spanning this native climatic range, (ii) that rate and efficiency of leaf nitrogen resorption would be associated with the conservation-acquisition trade-off, (iii) that the natural variation of resorption traits has strong genetic bases that have been selected in contrasting environments. The later implies that resorption traits display high heritability and significant associations with genetic variation.

Materials and methods

Plant material and growth conditions

We selected 121 natural genotypes from the 1001 GENOMES PROJECT list (Alonso-Blanco *et al.*, 2016), maximizing the geographic distribution and variance of the life cycle duration of the *A. thaliana* populations selected (Vasseur *et al.*, 2018a; Sartori *et al.*, 2019) (Supporting Information Table S1). We compiled 19 bioclimatic variable values to characterize the climate from the collection site of each genotype using the CHELSA database (http://chelsa-climate.org/). Eight times 121 pots (5×5×12 cm) were filled with a 1:1 mixture of sand and soil collected from the experimental field of the Centre d'Écologie Fonctionnelle et Évolutive (CEFE, Montpellier, France). This soil has a relatively low total nitrogen concentration (1.38±0.11 mg g^{-1}) (Kazakou *et al.*, 2007). A layer of 2-3 mm of organic compost (Neuhaus N2) was added to the soil surface in each pot to improve germination and seedling survival. Three to five seeds were sown on December 8th and 9th of 2016 on the soil surface of each pot. Pots were placed in the dark at 8°C for one month to ensure seed vernalization and then placed in a greenhouse at 18/15°C day/night with a 12.5 h photoperiod. Eight individual plants per genotype were randomly placed, spaced apart in a checkerboard to avoid self-shading, on forty-four trays split across four tables. Tables were rotated daily to reduce block effects within the greenhouse. Measurements started at bolting stage, i.e. apparition of the flowering bud, for each individual plant. At this moment, we marked the largest leaf fully exposed to light of each

individual plant. Aboveground parts of four replicates per genotype were harvested at bolting and kept in deionized water at 4°C for one night before conducting destructive measurements (see below). The four remaining replicates were used to perform non-destructive measurements on the marked leaf until its complete senescence (see below). We used the flowering time (FT), i.e. the number of days from germination to opening of the first flower as a proxy of the individual life cycle length.

Destructive measurements

The marked leaf of each plant individual was harvested at bolting, after plant rehydration, and placed in a test tube with deionized water for rehydration 24 h at 4°C. Marked leaves were then scanned to determine the leaf area (LA, mm²). Marked leaves were oven-dried at 70°C for 72 h to determine the leaf dry mass (DM, mg). Specific leaf area (SLA, $m^2\ kg^{-1}$) was calculated as the ratio between leaf area and leaf dry mass. A subset of 126 randomly selected dry leaves were ground individually to assess leaf nitrogen concentration (LNC, %) at bolting using the Pregl-Dumas method performed with a CHN Elemental Analyzer (Flash EA1112 Series, Thermo Finnigan, Milan, Italy).

Non-destructive measurements

Leaf area of the marked leaf of each tracked individual was determined two to three times a week from pictures taken with a smartphone (Microsoft Lumia 540®) equipped with an 8 Mpx camera and white plastic cube sticks on the flashlight as a light diffuser. Using an aluminum board, we made a small lightbox attached to the smartphone, designed to squeeze the leaves between a white support and a transparent piece of plastic (Fig. S1). Images were calibrated and leaf area was determined using ImageJ (Schneider *et al.*, 2012). Time-course measurements of the marked leaf optical properties were performed using a Near Infra-Red Spectrometer (LabSpec 4, ASD Inc.). Light absorbance of leaf tissues was recorded for the spectral region 350-2500 nm near the tip and at one edge of the leaves avoiding the midrib. Data represent leaf light absorbance for 2150 successive wavelengths, averaged for tip and edge (Fig S2). Marked leaves were harvested at complete senescence and all of them were ground individually (459 leaves in total) to assess leaf nitrogen concentration (LNC, %) as described above.

Leaf nitrogen dynamics

The procedure for N time course estimation is presented in Fig. S3. The first step was predicting SLA and LNC from spectral records. Wavelengths from the spectral records are considered as independent variables for the following analysis, despite the strong association between two successive wavelengths. We checked the presence of outlier spectra by computing a Mahalanobis distance on the coordinates of a principal component analysis (Whitfield *et al.*, 1987) and removed any spectrum exceeding the 95th quantile of the distances (11,250 remaining spectra). Samples collected at bolting and at complete senescence of the marked leaves were used as reference values to calibrate the models that predict leaf trait values at intermediate ages (LNC, 585 spectra; SLA, 882). We performed locally weighted partial least square regressions (Zavala-Ortiz *et al.*, 2020) using the measured SLA or LNC value as the predicted variable and the wavelength absorbance as the predictive variable. To select the best model parameters and spectra pre-treatments, we used a cross-validation method, which consisted in training the model on 70% of the reference values, then predicting the values of the remaining 30%. Best model pretreatments for both SLA and LNC were a Savitzky-Golay smoothing (Savitzky & Golay, 1964) with a 42 wavelengths window, a second order polynomial and first order derivative. Accuracy of the models was high for both SLA and LNC: the correlation coefficients of the predicted vs. measured values regression were higher than 0.95 (Fig. S4).

Data exploration suggested that temporal trajectories of SLA and LNC with leaf age followed a decreasing sigmoidal trend and leaf area followed a bell-shaped curve (Fig. 2). We therefore fitted time-course data using three different functions: gaussian, decreasing logistic and polynomial. Time-course trait variation was modeled using the function that minimized the error, estimated with the least square method. If none of the three functions fitted the data with a correlation coefficient higher than 0.75, the individual was removed from the analysis. Time-course of leaf dry mass (DM) and leaf nitrogen quantity (qN) were calculated as follows:

Eq.1 $DM = Area / SLA;$

Eq.2 $qN = LNC \times DM.$

We searched for outliers using a shape-clustering algorithm. Virtually all marked leaves showed decreasing sigmoidal trends of qN decrease that differed in amplitude and rate (N = 407, Fig. S5b). We observed a few leaves with sudden increases in qN at end of the leaf lifespan, a behavior that could arise from accumulating error through the estimation procedure or from

drastic changes in leaf properties; those individuals were removed from the klmShape clustering analysis (N=34, Fig. S5a). For each marked leaf we measured the maximum nitrogen resorption rate (RR_N, mg d^{-1}) as the maximum absolute value of the local slopes of qN dynamics obtained from the first derivative value at each time point. Second, we extracted the day and value of leaf maximum nitrogen quantity (dN_{max}, d; qN_{max}, mg) to estimate the nitrogen resorption efficiency (RE_N, %), i.e. the proportion of total nitrogen resorbed. Since a single leaf was tracked through time, there is no need for area and mass standardization (Heerwaarden *et al.*, 2003), and RE_N can be directly calculated as:

Eq.3 $$RE_N = (qN_{max} - qNmin) / qN_{max}.$$

Overall, the method we used to measure qN variation and related traits controls for dilution effects that may arise from leaf thickening, or from leaf mass and area increasing due to spectral pretreatments and precise daily mass and area tracking, respectively. Thus, any change in leaf N status reflects leaf N in and out fluxes.

Genome-wide association study

We performed a genome wide association study (GWAS) using the GEMMA software (Zhou & Stephens, 2012). The method uses the single nucleotide polymorphisms (SNPs) as predictors of the traits in a linear mixed model. A relatedness matrix was added to the model in order to account for population structure. From the genetic data available on the 1001 genomes project website (1001genomes.org), we excluded all variants with more than two possible alleles and all variants with more than 10% of missing values. Bonferroni significance threshold of $\alpha = 0.05$ was used to identify SNPs associated with the traits.

Genome scan for selection

We scanned for SNPs under selection using an F_{ST}-like method (Luu *et al.*, 2017). This method postulates that SNPs under selection contribute more to population structure than expected by neutral processes, such as genetic drift. The method uses a principal component analysis (PCA) to detect the population structure based on the genetic information. The scores of the variables (the SNPs here) reflect their contribution to the construction of the principal components of the PCA and are processed as p-values. Outliers in the contribution distribution are considered highly differentiated between populations and, by extension, under selection. This method had the advantage of considering the genotypes as part of large regional and continuous populations, well suited for *A. thaliana* genotypes (Horton *et al.*, 2012). We started

with the full set of 1,135 genotype sequences available on the 1001 genome project website (1001genomes.org) containing 12,883,854 variant loci. We pruned the data by keeping only the SNPs, loci and genotypes having less than 10% of missing data, which resulted in a 1,032 genotypes by 6,385,774 SNPs dataset. We then filtered genotypes by genetic distance using a 0.075 correlation coefficient limit. Final data contained 222 genotypes and 6,385,774 SNPs. We spotted outlier SNPs that reached the Bonferroni significance threshold of $\alpha = 0.05$. The SNPs that were significant in both the GWAS and the selection scan delineated relevant regions of the genome for further analyses. To account for the effect of linkage disequilibrium, we extended the detected windows by 10 Kb upstream and downstream significant SNPs (Kim *et al.*, 2007). Using The Arabidopsis Information Resource database (www.arabidopsis.org), we extracted the list and functions of genes carried by those sequences.

Statistical analysis

All statistical analyses but GWAS were performed using the R software (R Core Team, 2019, version 3.6.1).

The chemometric analyses were performed using the *rnirs* package (https://github.com/mlesnoff/rnirs). A clustering of N dynamics was performed using the *kmlShape* package (Genolini *et al.*, 2016).

We estimated trait broad-sense heritability (H^2) as the part of variance explained by the genotype by performing linear mixed models using the package *nlme* (Pinheiro *et al.*, 2020). We calculated trait genotype means by estimating the marginal means of the variables from linear mixed models including the genotype identity as a random effect and the experimental trails as fixed effects. The models were performed with the *lme* function from the *nlme* package, and the marginal means were computed with the *emmeans* function from the *emmeans* package (Searle *et al.*, 1980).

Mean comparisons were performed using a Student's *t*-test test with the *t.test* function. The scaling of RR_N to qN was tested using a standardized major axis (SMA) regression using the *smatr* package (Warton *et al.*, 2006). Given the importance of the life cycle length in driving adaptive strategies in *A. thaliana*, we analyzed the RR_N-SLA and RE_N-SLA relationships by controlling for the flowering time using partial correlations performed using the *ppcor* R package (Kim, 2015).

Genome scans for selection were performed using the *PCAdapt* package (Luu *et al.*, 2017) and q-values were calculated using the *q-value* package (Storey *et al.*, 2004).

Results

Leaf trait dynamics

On average (± se), the marked leaves reached their maximum area 16.7 ± 9.4 days after bolting (Fig. 2). This indicates that measurements started before leaves were fully expanded. Leaf area decreased until complete senescence, following a bell-shaped curve. Specific leaf area (SLA) and leaf nitrogen concentration (LNC) reached their maximum values significantly earlier than leaf area (both $P < 0.01$) and then decreased following a sigmoidal curve. The N peak occurred on average 10.3 ± 6.7 days after bolting. The LA peak occurred significantly later than the N peak ($P < 0.01$) and on average 16.7 ± 9.4 days after the onset of measurements. The maximum qN decrease (RR_N measurement day) occurred significantly later than the LA peak ($P < 0.01$) and on average 21.9 ± 9.7 days after bolting. Finally, the peak of dry mass occurred significantly later than maximum leaf area ($P < 0.01$) and on average 23.4 ± 9.8 days after bolting.

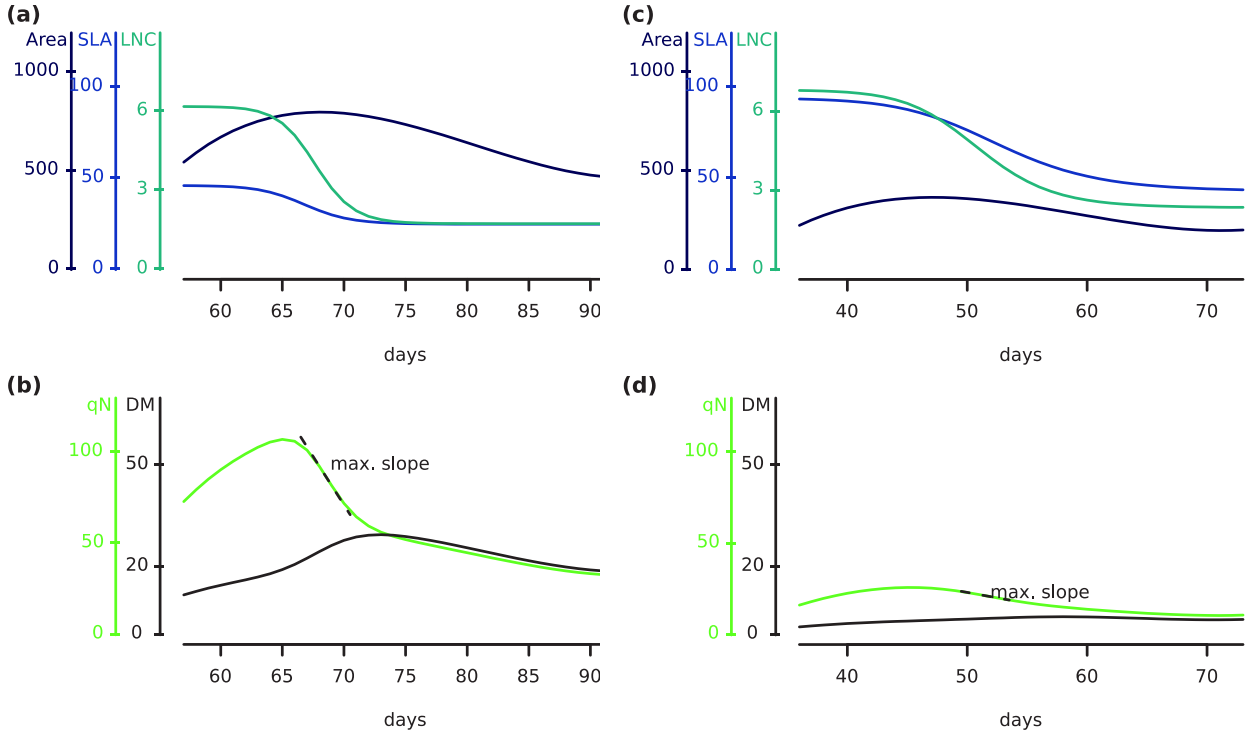

Figure 2: Observed temporal variability of leaf properties of a slow-growing plant (a, b) versus a fast-growing plant (c, d). The Y-axes represent the following traits: Area, leaf area (mm^2); SLA, specific leaf area ($m^2\ kg^{-1}$); LNC, leaf nitrogen concentration (%); qN, nitrogen quantity (mg); DM, leaf dry mass (mg). The X-axes represent the days after germination along which the onset of trait recording vary, depending on plant slow-fast strategies.

Trait variability and heritability

N resorption efficiency (mean RE_N = 64.9 ± 14.5 %) and resorption rate (mean RR_N = 4.1 ± 3.5 mg d^{-1}) displayed significant variation among natural genotypes and had a broad-sense heritability (H^2) of 0.20 and 0.76, respectively. Traits related to the structure and composition of the leaves were highly heritable: DM (12.4 ± 6.2 mg; H^2 = 0.64), LA (496 ± 169 mm^2; H^2 = 0.61), SLA (55.7 ± 13.6 mm^2 mg^{-1}; H^2 = 0.67), maximum nitrogen quantity (48.4 ± 20.9 mg, H^2 = 0.72). Conversely, LNC heritability was surprisingly low (5.4 ± 0.7%, H^2 ~ 0.11). Flowering time (FT) was the most heritable trait (52.6 ± 13.8 d, H^2 ~ 0.89).

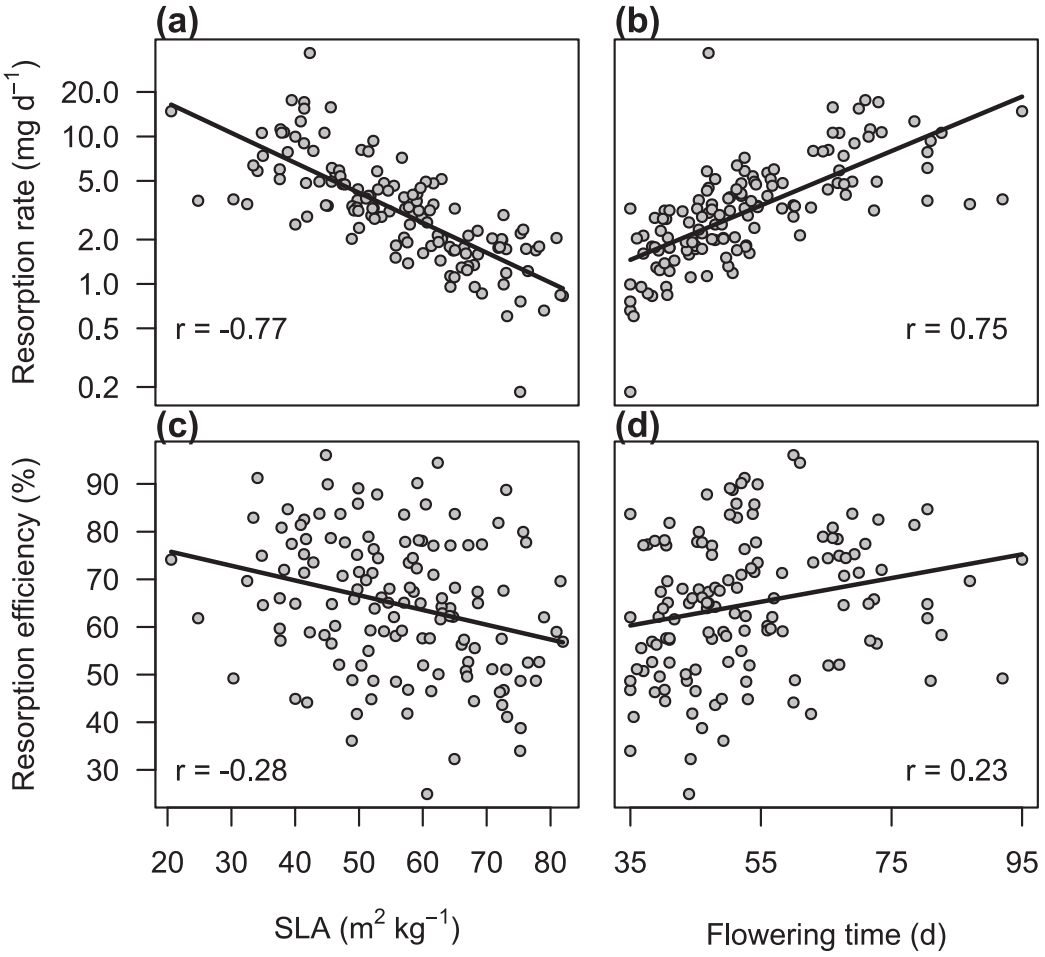

Figure 3: Relationships between nitrogen resorption, specific leaf area, and flowering time across natural genotypes of *A. thaliana*. Each dot represents the average trait value of a natural genotype (grey circles; n = 121). Lines represent significant linear relationships at $P < 0.05$. Pearson's correlation coefficients are reported for each relationship. Resorption rate is represented on a log_{10}-scale.

Relationships between nitrogen resorption and other plant traits

Across ecotypes, RR_N was negatively associated with SLA (r = –0.77, $P < 0.01$) and positively associated with FT (r = 0.75, P < 0.01) (Fig. 3a, b). The negative relationship of RR_N with SLA was independent of FT (partial correlation $r = –0.31$, $P < 0.001$). Further, RE_N was negatively associated with SLA (r = –0.28, $P < 0.01$) and positively associated with FT (r = 0.23, $P < 0.01$) (Fig. 3c,d), and the relationship of RE_N and SLA was also independent of FT (partial correlation r = –0.16, $P = 0.05$).

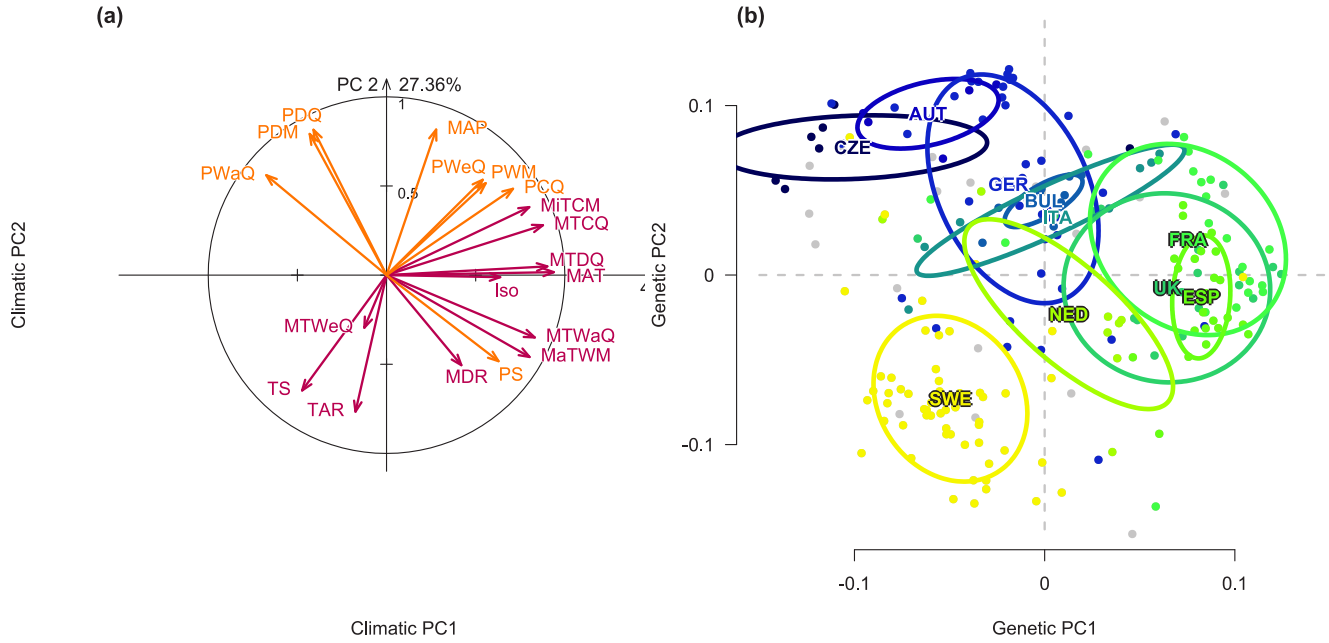

Figure 4: Climatic and genetic differentiation of *Arabidopsis thaliana* populations. (a) Correlation circle of a principal component analysis performed on a matrix composed of the 19 climatic variables obtained from the CHELSA database and the genotype collecting sites (n = 140). Climatic variables related to temperature are represented in red and those related to precipitation are represented in orange. (b) Score plot of a principal component analysis performed on the genetic data obtained from the 1001 genomes project database and the genotypes (n = 222). Each dot represents a genotype, and ellipses represent bivariate normal density contour of the best represented countries. Abbreviations: MAP; Mean Annual Temperature, MDR; Mean Diurnal Range, Iso; Isothermality, TS; Temperature Seasonality, MaTWM; Max Temperature of Warmest Month, MiTCM; Min Temperature of Coldest Month, TAR; Temperature Annual Range, MTWeQ; Mean Temperature of Wettest Quarter, MTDQ; Mean Temperature of Driest Quarter, MTWaQ; Mean Temperature of Warmest Quarter, MTCQ; Mean Temperature of Coldest Quarter, MAP; Mean Annual Precipitation, PWM; Precipitation of Wettest Month, PDM; Precipitation of Driest Month, PS; Precipitation Seasonality, PWeQ; Precipitation of Wettest Quarter, PDQ; Precipitation of Driest Quarter, PWaQ; Precipitation of Warmest Quarter; PCQ; Precipitation of Coldest Quarter; CZE, Czech Republic; AUT, Austria; GER, Germany; BUL, Bulgaria; ITA, Italy; UK, United Kingdom; FRA, France; ESP, Spain; NED, Netherlands; SWE, Sweden.

Axes of climatic and genetic population differentiation

The two first principal components of the climatic PCA accounted for 68% of the variation of the 19 CHELSA climatic variables (Fig. 4a). The first axis was mainly driven by the mean annual temperature, the mean temperature of the driest and the warmest quarter, and overall increased with increasing temperature. The second axis was mainly driven by the mean annual precipitation and the precipitation of the driest month and driest quarter, and it increased overall with increasing precipitation. The genetic PCA (PCAdapt) revealed that *A. thaliana* genotypes were differentiated along two major axes of variation following their geographical location (Fig. 4b). The first axis (Genetic PC1) described the Eastern Europe-Western Europe differentiation, and the second axis (Genetic PC2) described the Southern Europe-Northern Europe differentiation of the regional populations.

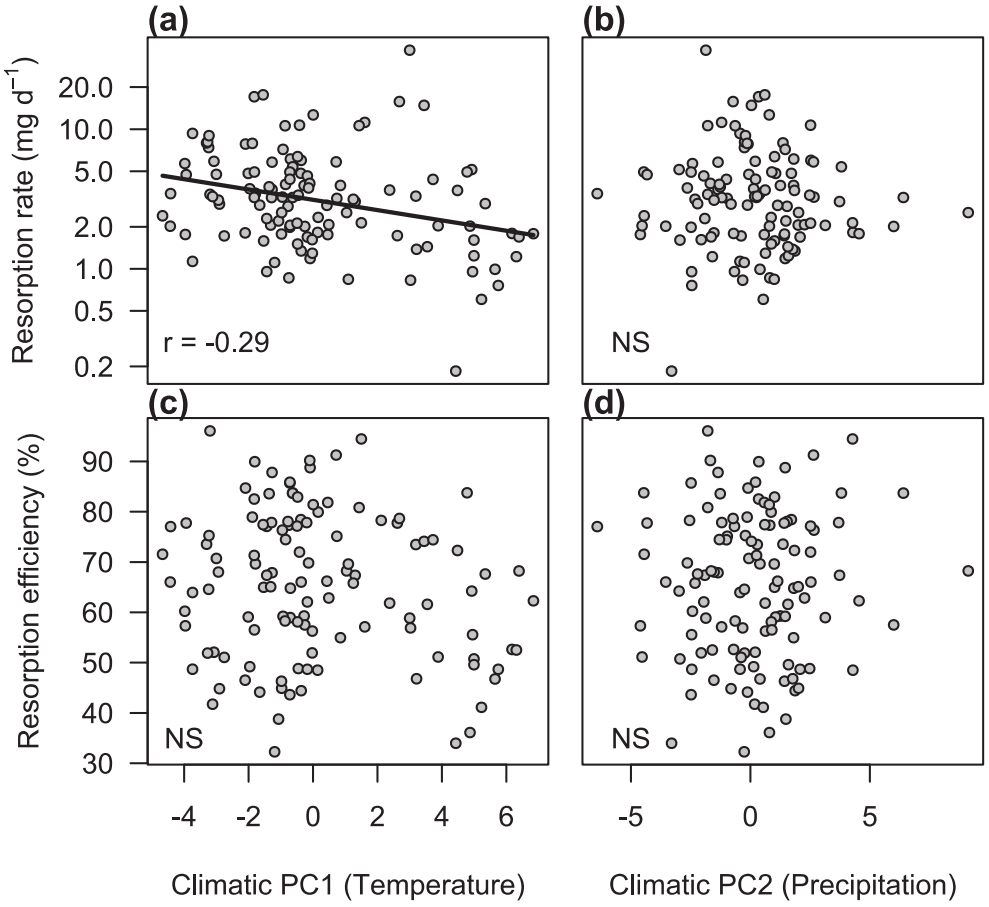

Figure 5: Relationships between the first principal components of climate variation of the collecting sites and resorption. Each dot represents the average value of a natural genotype (n = 121) of (a, b) resorption rate (log_{10}-scale) and (c, d) resorption efficiency as a function of climatic PCs scores from a principal component analysis performed on 19 climatic variables of the genotypes collecting sites (Fig. 4a). The values of PC1 and PC2 increase with increasing temperature and precipitation, respectively.

Adaptation cues and climatic drivers of resorption components

RR_N was negatively associated with increasing temperature of the native climate of the genotype (r = –0.29, $P < 0.05$) and was uncorrelated with average precipitation at the genotype collecting site (Fig. 5a,b). Resorption efficiency was not related to site temperature nor precipitation (Fig. 5c,d). The genome wide association study (GWAS) revealed 197 single nucleotide polymorphisms (SNPs) significantly associated with RR_N (Fig. 6a). Consistent with its low heritability level, we found no significant genetic association with RE_N (Fig. S6). From the genome scan for selection, none of the SNPs that contributed to the Eastern Europe-Western Europe differentiation were shared with those identified in the GWAS of RR_N. We detected 1,661 SNPs that contributed more than expected by neutral processes to the construction of the Southern Europe-Northern Europe axis (Fig. 6b). Among them, three consecutive SNPs were shared with the GWAS of RR_N. These SNPs delineated a region going from the 6,754,500 bp to the 6,775,500 bp of the fourth chromosome. Seven genes are coded in this region (see Supporting Information Table S2) including AT4G11070, a protein-coding gene called WRKY41, member of the WRKY transcription factor family.

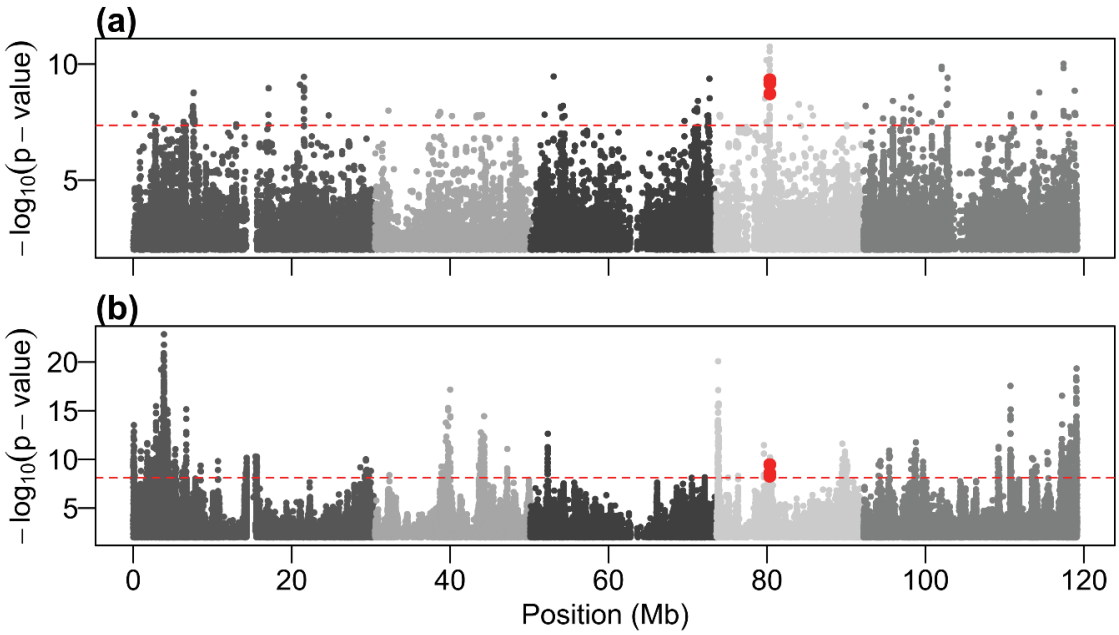

Figure 6: The polymorphism of a short sequence of Arabidopsis thaliana genome is associated with the resorption rate variation and is highly differentiated between populations. Panels are Manhattan plots, (a) representing the strength of the association between each single nucleotide (grey dots) polymorphism and the resorption rate variation, and (b) representing the contribution of each single nucleotide polymorphism on the genetic differentiation of Arabidopsis thaliana populations. Red dashed lines represent the significance threshold calculated with the Bonferroni method. Shades of grey delineate the five A. thaliana chromosomes.

Discussion

Historically, plant nutrient resorption is commonly evaluated through the outcome of the resorption process, i.e. resorption efficiency (Killingbeck, 1986). This approach meets a need to establish the economic record of leaves (Bloom *et al.*, 1985; Wright *et al.*, 2004). Consistent with previous interspecific comparisons, resorption efficiency in *A. thaliana* was high on average (> 60%) (Kazakou *et al.*, 2007) and showed a medium value of broad-sense heritability (< 30%) (e.g. Mikola *et al.*, 2018). This result suggests that, despite its theoretical importance in the context of leaf resource economics, resorption efficiency may not have the genetic basis to respond to natural selection. The main driver of nitrogen resorption is the strength of the nitrogen demand from newly formed leaves (Harper & Sellek, 1987), and, especially in annual species such as *A. thaliana*, growing flowers and seeds (Havé *et al.*, 2017). Thus, we hypothesized that selection on resorption capacity may not act on traits that maximize effectiveness at the leaf level. Instead, selection would act on traits that allow a response at the plant level to meet the nitrogen demand of surviving and growing tissues. Such a demand can be uncoupled from the individual capacity of leaves. Depending on the plant growth strategy, it might be advantageous for the plant to remobilize leaf nitrogen stocks more or less quickly. In this context, the rate of nitrogen resorption proves to be a promising candidate for describing differences in resorption strategies between genotypes. To our knowledge, this is the first time such a rate of nitrogen resorption had been reported. Using an innovative method based on the near infrared absorbance of leaf tissues (Vilmus *et al.*, 2014), we tracked daily changes in nitrogen quantity in living leaves. Resorption rate varied by a factor of 12 among genotypes and was highly heritable (broad-sense heritability = 76%). This result suggests a need for studies exploring the genetic, physiological, and morphological variations responsible for time course variations in nitrogen quantity. Additionally, we provide new insights about changes in leaf properties during leaf senescence. Previous studies reported that in *A. thaliana*, leaf senescence begins as soon as leaves reach their full adult size and maximum sugar content value (Diaz *et al.*, 2005, 2008). Diaz *et al.* observed that nitrogen, starch, protein, and chlorophyll content decrease, and leaf yellowing starts as soon as leaves reach full expansion. Our results do not support this assertion; among the 121 natural *A. thaliana* genotypes studied, leaf nitrogen concentration started to decrease on average a few days before leaves were fully expanded, suggesting that first signs of senescence occur before complete leaf maturity. This unexpected pattern may arise for two reasons: (i) the leaf N status does not reflects the photosynthetic maturity of the leaf; (ii) morphological and physiological leaf maturity are asynchronous. First,

studies showed that leaves build up N reserves at their juvenile stage and N remobilization is triggered by transition to reproductive stage (Santiago & Tegeder, 2017). Thus, the initial decrease in leaf N quantity during leaf expansion might be the result of N reallocation independent from leaf senescence. Second, leaf growth is the result of two uncoupled developmental processes: cell expansion and cell division (Tsiantis & Hay, 2003). Cell expansion is mainly constrained by water availability while cell division depends on photosynthates (Körner, 2013), suggesting that leaf growth can still occur during senescence in well-watered conditions despite the drop of carbon assimilation. Moreover, leaf dry mass still increased after the decline of leaf expansion and leaf nitrogen concentration in our dataset, consistently with the late increase in sugar concentration in several *A. thaliana* recombinant inbred lines (Diaz *et al.*, 2005). These observations challenge our conception of leaf nitrogen and carbon in- and out-fluxes during leaf ageing. Our study was limited to tracking a single leaf per plant and during the second half of its lifespan. More studies are needed to better understand how the dynamics of leaf properties are driven by plant life history events such as the production of new leaves and reproductive organs.

Given its importance for plant resource economics, nitrogen acquisition and conservation strategies have been included in a slow-fast syndrome at both plant and leaf levels (Reich, 2014). However, previous interspecific explorations of the linkage between resorption efficiency and leaf economics traits did not report clear signals (Kazakou *et al.*, 2007; Freschet *et al.*, 2010). As expected, our results showed that high resorption efficiency was associated with low specific leaf area and late maturity corresponding to a slow-leaf and slow-plant syndromes (Sartori *et al.*, 2019), respectively. Conversely, fast syndromes were characterized by low resorption efficiency. However, correlations were weak, indicating that for a given value of resorption efficiency, plants expressed a large range of specific leaf area and flowering time values.. By contrast, resorption rate correlated strongly with the plant and leaf syndromes in our dataset. The fact that slow strategies at the plant and leaf level were characterized by high leaf resorption rates contradicts our initial expectations. Leaves from fast-growing plants exhibited a slow decrease in nitrogen quantity while leaves from slow-growing plants had fast nitrogen resorption within a short time. Fast growing genotypes reach sexual maturity earlier with a lower plant biomass and leaf number than slow growing genotypes (Vasseur *et al.*, 2018a), consistent with a slow-fast syndrome (Salguero-Gómez *et al.*, 2016; Dammhahn *et al.*, 2018). Thus, the rate of leaf nitrogen resorption might be adjusted to the plant-level nitrogen demand. As reported by Diaz and colleagues (2005), the time course of leaf senescence is correlated with

the total number of leaves that compose the rosette in *A. thaliana*. We hypothesize that large plants composed of numerous leaves impose a strong nitrogen demand on senescent leaves. In addition, as we measured traits after bolting, the construction of reproductive organs may impose a supplementary nitrogen demand on leaves. Slow plant strategies are expected to produce protein-rich seeds (Westoby, 1998) that require more nitrogen than fast plant seeds. This strong source-sink relationship suggests that leaf-level resorption capacity can be uncoupled from leaf-level resource use strategies and should be considered relative to whole-plant functioning. Future experimental studies measuring nitrogen transfers between organs of the whole individuals are needed to properly test these assumptions.

Our results did not show any correlation between nitrogen resorption efficiency and temperature or precipitation, contrary to previous observations in interspecific biogeographic meta-analyses (Yuan & Chen, 2009; Drenovsky *et al.*, 2019). The most parsimonious explanation is that the effect of the environment on the resorption efficiency is mediated through phenotypic plasticity, rather than local adaptation (consistent with our lack of heritability for this trait), and growing plants in homogeneous conditions would have removed such influence of phenotypic plasticity. Since the resorption efficiency is known to vary depending on the growing conditions (Chapin, 1980), phenotypic plasticity could also be responsible for the lack of relationship in our dataset. By contrast, the rate of nitrogen resorption covaried with climate: high rates of nitrogen resorption were expressed by genotypes originating from cooler habitats. Despite the importance of microclimate for *A. thaliana* local adaptation (Brachi *et al.*, 2013), annual temperature may reflect the average growing conditions that the populations encounter. Therefore, environmental variables capturing spatially imprecise data are still considered approximate estimators of stress that plants experience (Borgy *et al.*, 2017). The relatively recent migration of *A. thaliana* toward Scandinavia was accompanied by allele fixation conferring resistance to harsh environmental conditions imposed by coldness (Krämer, 2015; Exposito-Alonso *et al.*, 2018). Such climatic constraints should have selected for trait values characteristic of a conservative syndrome (Borgy *et al.*, 2017), such as low LES scores (Sartori *et al.*, 2019), and trait values determinant for leaf senescence and lifespan such as resorption capacity. However, it will be important to account for variation in local soil resource availability to further explore the biogeographical determinants of the different facets of resorption ability (Drenovsky *et al.*, 2019). Indeed, nutrient poor environments are supposed to select for traits reducing nutrient losses (Aerts & Chapin, 1999) and should thus also regulate variation in the rate of nutrient resorption.

The high heritability of nitrogen resorption rate was reflected by the numerous genetic associations detected along the *A. thaliana* genome. To filter for relevant associations, we conducted an independent screening for loci under selection based on the genetic structure of *A. thaliana* populations. We identified major axes of genetic differentiation that correspond to the geographic differentiation of regional *A. thaliana* populations. Interestingly, one locus showed simultaneously significant association with nitrogen resorption rate and significant effect on the genetic differentiation along the latitudinal distribution of the species. The locus notably codes for a member of the WRKY transcription factor family, called WRKY41. WRKY proteins are transcription factors that play roles in diverse, important processes such as germination, senescence, and response to stresses (Rushton *et al.*, 2010). They represent the second largest family of genes expressed during leaf senescence (Guo *et al.*, 2004). Previous studies showed that deactivation and overexpression induce delayed and accelerated leaf senescence, respectively (Miao *et al.*, 2004) and affect leaf lifespan (Doll *et al.*, 2020). While, in this study, our ambition was not to identify genes that are determinant for the resorption capacity in *A. thaliana*, this result is a rare convergence between genomic and ecological findings. It demonstrates the role of nitrogen resorption in leaf senescence and lifespan, and its importance for local adaptation.

Overall, our results emphasize the ecological and evolutionary importance of a leaf nitrogen resorption component that has been poorly explored so far. Combined with genetic and climatic data, our findings reveal that high rates of nitrogen resorption, rather than high efficiency, are favored toward the northern and colder region of the *A. thaliana* distribution. We provide evidence that the resorption rate is integrated in leaf and plant level resource use strategies and growth syndrome, suggesting its importance for better plant fitness characterization. Next steps will be to explore the anatomical and molecular determinants of the resorption rate as done for nitrogen resorption efficiency, such as the leaf vein architecture (Zhang *et al.*, 2015) and the enzymes responsible for N-bearing molecules catalysis and transport (Moison *et al.*, 2018). Finally, future studies might also explore the relative role of soil nitrogen availability and plant nitrogen demand on the time-course of nitrogen at the organ and plant levels. The combined use of comparative ecology, quantitative genetics and population genetics is a promising avenue to understand the role of physiological constraints and trait syndromes in plant adaptation.

Acknowledgements

We are grateful to Thierry Mathieu, David Degueldre, and Pauline Durbin from the TE platform of the Labec CEMEB for their technical assistance. We also thank Pascal Tillard for his assistance with CHN measurements. This work was supported by the European Research Council (ERC) ('CONSTRAINTS': grant ERC-StG-2014-639706-CONSTRAINTS).

References

Achat DL, Pousse N, Nicolas M, Augusto L. **2018**. Nutrient remobilization in tree foliage as affected by soil nutrients and leaf life span. *Ecological Monographs* **88**: 408–428.

Aerts R, Chapin FS. **1999**. The Mineral Nutrition of Wild Plants Revisited: A Re-evaluation of Processes and Patterns. In: Fitter AH, Raffaelli DG, eds. Advances in Ecological Research. Academic Press, 1–67.

Alonso-Blanco C, Andrade J, Becker C, Bemm F, Bergelson J, Borgwardt KM, Cao J, Chae E, Dezwaan TM, Ding W, *et al.* 2016. 1,135 Genomes Reveal the Global Pattern of Polymorphism in Arabidopsis thaliana. *Cell* **166**: 481–491.

Berendse F, Aerts R. **1987**. Nitrogen-Use-Efficiency: A Biologically Meaningful Definition? *Functional Ecology* **1**: 293–296.

Bloom AJ, Chapin FS, Mooney HA. **1985**. Resource Limitation in Plants-An Economic Analogy. *Annual Review of Ecology and Systematics* **16**: 363–392.

Borgy B, Violle C, Choler P, Denelle P, Munoz F, Kattge J, Lavorel S, Loranger J, Amiaud B, Bahn M, *et al.* 2017. Plant community structure and nitrogen inputs modulate the climate signal on leaf traits. *Global Ecology and Biogeography* **26**: 1138–1152.

Brachi B, Aimé C, Glorieux C, Cuguen J, Roux F. **2012**. Adaptive Value of Phenological Traits in Stressful Environments: Predictions Based on Seed Production and Laboratory Natural Selection. *PLOS ONE* **7**: e32069.

Brachi B, Villoutreix R, Faure N, Hautekèete N, Piquot Y, Pauwels M, Roby D, Cuguen J, Bergelson J, Roux F. **2013**. Investigation of the geographical scale of adaptive phenological variation and its underlying genetics in *Arabidopsis thaliana*. *Molecular Ecology* **22**: 4222–4240.

Campanella MV, Bertiller MB. **2011**. Is N-resorption efficiency related to secondary compounds and leaf longevity in coexisting plant species of the arid Patagonian Monte, Argentina? *Austral Ecology* **36**: 395–402.

Chapin FS. **1980**. The Mineral Nutrition of Wild Plants. *Annual Review of Ecology and Systematics* **11**: 233–260.

Dammhahn M, Dingemanse NJ, Niemelä PT, Réale D. **2018**. Pace-of-life syndromes: a framework for the adaptive integration of behaviour, physiology and life history. *Behavioral Ecology and Sociobiology* **72**.

Diaz C, Lemaître T, Christ A, Azzopardi M, Kato Y, Sato F, Morot-Gaudry J-F, Dily FL, Masclaux-Daubresse C. **2008**. Nitrogen Recycling and Remobilization Are Differentially Controlled by Leaf Senescence and Development Stage in Arabidopsis under Low Nitrogen Nutrition. *Plant Physiology* **147**: 1437–1449.

Diaz C, Purdy S, Christ A, Morot-Gaudry J-F, Wingler A, Masclaux-Daubresse C. **2005**. Characterization of Markers to Determine the Extent and Variability of Leaf Senescence in Arabidopsis. A Metabolic Profiling Approach. *Plant Physiology* **138**: 898–908.

Doll J, Muth M, Riester L, Nebel S, Bresson J, Lee H-C, Zentgraf U. **2020**. Arabidopsis thaliana WRKY25 Transcription Factor Mediates Oxidative Stress Tolerance and Regulates Senescence in a Redox-Dependent Manner. *Frontiers in Plant Science* **10**.

Drenovsky RE, Pietrasiak N, Short TH. **2019**. Global temporal patterns in plant nutrient resorption plasticity. *Global Ecology and Biogeography* **28**: 728–743.

Ecarnot M, Compan F, Roumet P. **2013**. Assessing leaf nitrogen content and leaf mass per unit area of wheat in the field throughout plant cycle with a portable spectrometer. *Field Crops Research* **140**: 44–50.

Exposito-Alonso M, Vasseur F, Ding W, Wang G, Burbano HA, Weigel D. **2018**. Genomic basis and evolutionary potential for extreme drought adaptation in Arabidopsis thaliana. *Nature Ecology & Evolution* **2**: 352–358.

Freschet GT, Cornelissen JHC, Logtestijn RSP van, Aerts R. **2010**. Substantial nutrient resorption from leaves, stems and roots in a subarctic flora: what is the link with other resource economics traits? *New Phytologist* **186**: 879–889.

Genolini C, Ecochard R, Benghezal M, Driss T, Andrieu S, Subtil F. **2016**. kmlShape: An Efficient Method to Cluster Longitudinal Data (Time-Series) According to Their Shapes (C-H Huang, Ed.). *PLOS ONE* **11**: e0150738.

Guo Y, Cai Z, Gan S. **2004**. Transcriptome of Arabidopsis leaf senescence. *Plant, Cell & Environment* **27**: 521–549.

Harper JL, Sellek C. **1987**. The effects of severe mineral nutrient deficiencies on the demography of leaves. *Proceedings of the Royal Society of London. Series B. Biological Sciences* **232**: 137–157.

Havé M, Marmagne A, Chardon F, Masclaux-Daubresse C. **2017**. Nitrogen remobilization during leaf senescence: lessons from Arabidopsis to crops. *Journal of Experimental Botany* **68**: 2513–2529.

Heerwaarden LMV, Toet S, Aerts R. **2003**. Current measures of nutrient resorption efficiency lead to a substantial underestimation of real resorption efficiency: facts and solutions. *Oikos* **101**: 664–669.

Horton MW, Hancock AM, Huang YS, Toomajian C, Atwell S, Auton A, Muliyati NW, Platt A, Sperone FG, Vilhjálmsson BJ, *et al.* 2012. Genome-wide patterns of genetic variation in worldwide Arabidopsis thaliana accessions from the RegMap panel. *Nature Genetics* **44**: 212–216.

Kazakou E, Garnier E, Navas M-L, Roumet C, Collin C, Laurent G. **2007**. Components of nutrient residence time and the leaf economics spectrum in species from Mediterranean old-fields differing in successional status. *Functional Ecology* **21**: 235–245.

Killingbeck KT. **1986**. The Terminological Jungle Revisited: Making a Case for Use of the Term Resorption. *Oikos* **46**: 263.

Kim S. **2015**. ppcor: An R Package for a Fast Calculation to Semi-partial Correlation Coefficients. *Communications for statistical applications and methods* **22**: 665–674.

Kim S, Plagnol V, Hu TT, Toomajian C, Clark RM, Ossowski S, Ecker JR, Weigel D, Nordborg M. **2007**. Recombination and linkage disequilibrium in *Arabidopsis thaliana*. *Nature Genetics* **39**: 1151–1155.

Körner C. **2013**. Growth Controls Photosynthesis – Mostly. *Nova Acta Leopoldina* **114**: 273–283.

Krämer U. **2015**. Planting molecular functions in an ecological context with Arabidopsis thaliana. *eLife* **4**: e06100.

Lasky JR, Des Marais DL, McKAY JK, Richards JH, Juenger TE, Keitt TH. **2012**. Characterizing genomic variation of *Arabidopsis thaliana* : the roles of geography and climate: GEOGRAPHY, CLIMATE AND ARABIDOPSIS GENOMICS. *Molecular Ecology* **21**: 5512–5529.

Lovell JT, Juenger TE, Michaels SD, Lasky JR, Platt A, Richards JH, Yu X, Easlon HM, Sen S, McKay JK. **2013**. Pleiotropy of FRIGIDA enhances the potential for multivariate adaptation. *Proceedings of the Royal Society of London B: Biological Sciences* **280**: 20131043.

Luu K, Bazin E, Blum MGB. **2017**. *pcadapt* : an R package to perform genome scans for selection based on principal component analysis. *Molecular Ecology Resources* **17**: 67–77.

Masclaux-Daubresse C, Chardon F. **2011**. Exploring nitrogen remobilization for seed filling using natural variation in Arabidopsis thaliana. *Journal of Experimental Botany* **62**: 2131–2142.

Mendez-Vigo B, Pico FX, Ramiro M, Martinez-Zapater JM, Alonso-Blanco C. **2011**. Altitudinal and Climatic Adaptation Is Mediated by Flowering Traits and FRI, FLC, and PHYC Genes in Arabidopsis. *PLANT PHYSIOLOGY* **157**: 1942–1955.

Miao Y, Laun T, Zimmermann P, Zentgraf U. **2004**. Targets of the WRKY53 transcription factor and its role during leaf senescence in Arabidopsis. *Plant Molecular Biology* **55**: 853–867.

Mikola J, Silfver T, Paaso U, Possen BJMH, Rousi M. **2018**. Leaf N resorption efficiency and litter N mineralization rate have a genotypic tradeoff in a silver birch population. *Ecology* **99**: 1227–1235.

Mitchell-Olds T. **2001**. Arabidopsis thaliana and its wild relatives: a model system for ecology and evolution. *Trends in Ecology & Evolution* **16**: 693–700.

Moison M, Marmagne A, Dinant S, Soulay F, Azzopardi M, Lothier J, Citerne S, Morin H, Legay N, Chardon F, *et al.* 2018. Three cytosolic glutamine synthetase isoforms localized

in different-order veins act together for N remobilization and seed filling in Arabidopsis. *Journal of Experimental Botany* **69**: 4379–4393.

Pinheiro J, Bates D, DebRoy S, Sarkar D, R Core Team. **2020**. *nlme: Linear and Nonlinear Mixed Effects Models*.

R Core Team. **2019**. *R: A Language and Environment for Statistical Computing*. Vienna, Austria: R Foundation for Statistical Computing.

Reich PB. **2014**. The world-wide 'fast–slow' plant economics spectrum: a traits manifesto. *Journal of Ecology* **102**: 275–301.

Reich PB, Walters MB, Ellsworth DS. **1991**. Leaf age and season influence the relationships between leaf nitrogen, leaf mass per area and photosynthesis in maple and oak trees. *Plant, Cell & Environment* **14**: 251–259.

Rushton PJ, Somssich IE, Ringler P, Shen QJ. **2010**. WRKY transcription factors. *Trends in Plant Science* **15**: 247–258.

Salguero-Gómez R, Jones OR, Jongejans E, Blomberg SP, Hodgson DJ, Mbeau-Ache C, Zuidema PA, de Kroon H, Buckley YM. **2016**. Fast–slow continuum and reproductive strategies structure plant life-history variation worldwide. *Proceedings of the National Academy of Sciences* **113**: 230–235.

Santiago JP, Tegeder M. **2017**. Implications of nitrogen phloem loading for carbon metabolism and transport during Arabidopsis development. *Journal of Integrative Plant Biology* **59**: 409–421.

Sartori K, Vasseur F, Violle C, Baron E, Gerard M, Rowe N, Ayala-Garay O, Christophe A, Jalón LG de, Masclef D, *et al.* 2019. Leaf economics and slow-fast adaptation across the geographic range of Arabidopsis thaliana. *Scientific Reports* **9**: 10758.

Savitzky Abraham, Golay MJE. **1964**. Smoothing and Differentiation of Data by Simplified Least Squares Procedures. *Analytical Chemistry* **36**: 1627–1639.

Schmalenbach I, Zhang L, Ryngajllo M, Jiménez-Gómez JM. **2014**. Functional analysis of the Landsberg erecta allele of FRIGIDA. *BMC Plant Biology* **14**: 1.

Schneider CA, Rasband WS, Eliceiri KW. **2012**. NIH Image to ImageJ: 25 years of image analysis. *Nature Methods* **9**: 671–675.

Searle SR, Speed FM, Milliken GA. **1980**. Population Marginal Means in the Linear Model: An Alternative to Least Squares Means. *The American Statistician* **34**: 216–221.

Storey JD, Taylor JE, Siegmund D. **2004**. Strong control, conservative point estimation and simultaneous conservative consistency of false discovery rates: a unified approach. *Journal of the Royal Statistical Society: Series B (Statistical Methodology)* **66**: 187–205.

Tsiantis M, Hay A. **2003**. Comparative plant development: the time of the leaf? *Nature Reviews Genetics* **4**: 169–180.

Vasseur F, Exposito-Alonso M, Ayala-Garay OJ, Wang G, Enquist BJ, Vile D, Violle C, Weigel D. **2018a**. Adaptive diversification of growth allometry in the plant *Arabidopsis thaliana*. *Proceedings of the National Academy of Sciences* **115**: 3416–3421.

Vasseur F, Sartori K, Baron E, Fort F, Kazakou E, Segrestin J, Garnier E, Vile D, Violle C. **2018b**. Climate as a driver of adaptive variations in ecological strategies in Arabidopsis thaliana. *Annals of Botany* **122**: 935–945.

Vasseur F, Violle C, Enquist BJ, Granier C, Vile D. **2012**. A common genetic basis to the origin of the leaf economics spectrum and metabolic scaling allometry. *Ecology Letters* **15**: 1149–1157.

Vilmus I, Ecarnot M, Verzelen N, Roumet P. **2014**. Monitoring Nitrogen Leaf Resorption Kinetics by Near-Infrared Spectroscopy during Grain Filling in Durum Wheat in Different Nitrogen Availability Conditions. *Crop Science* **54**: 284–296.

Warton DI, Wright IJ, Falster DS, Westoby M. **2006**. Bivariate line-fitting methods for allometry. *Biological Reviews* **81**: 259.

Westoby M. **1998**. A leaf-height-seed (LHS) plant ecology strategy scheme. *Plant and Soil* **199**: 213–227.

Whitfield RG, Gerger ME, Sharp RL. **1987**. Near-Infrared Spectrum Qualification via Mahalanobis Distance Determination. *Applied Spectroscopy* **41**: 1204–1213.

Wright IJ, Reich PB, Westoby M, Ackerly DD, Baruch Z, Bongers F, Cavender-Bares J, Chapin T, Cornelissen JHC, Diemer M, *et al.* 2004. The worldwide leaf economics spectrum. *Nature* **428**: 821–827.

Yuan ZY, Chen HYH. **2009**. Global-scale patterns of nutrient resorption associated with latitude, temperature and precipitation. *Global Ecology and Biogeography* **18**: 11–18.

Yuan ZY, Chen HYH. **2010**. Changes in nitrogen resorption of trembling aspen (Populus tremuloides) with stand development. *Plant and Soil* **327**: 121–129.

Zavala-Ortiz DA, Ebel B, Li M-Y, Barradas-Dermitz DM, Hayward-Jones PM, Aguilar-Uscanga MG, Marc A, Guedon E. **2020**. Interest of locally weighted regression to overcome nonlinear effects during in situ NIR monitoring of CHO cell culture parameters and antibody glycosylation. *Biotechnology Progress* **36**: e2924.

Zhang J-L, Zhang S-B, Chen Y-J, Zhang Y-P, Poorter L. **2015**. Nutrient resorption is associated with leaf vein density and growth performance of dipterocarp tree species (S Bonser, Ed.). *Journal of Ecology* **103**: 541–549.

Zhou X, Stephens M. **2012**. Genome-wide efficient mixed-model analysis for association studies. *Nature Genetics* **44**: 821–824.

SUPLEMENTAL INFORMATION

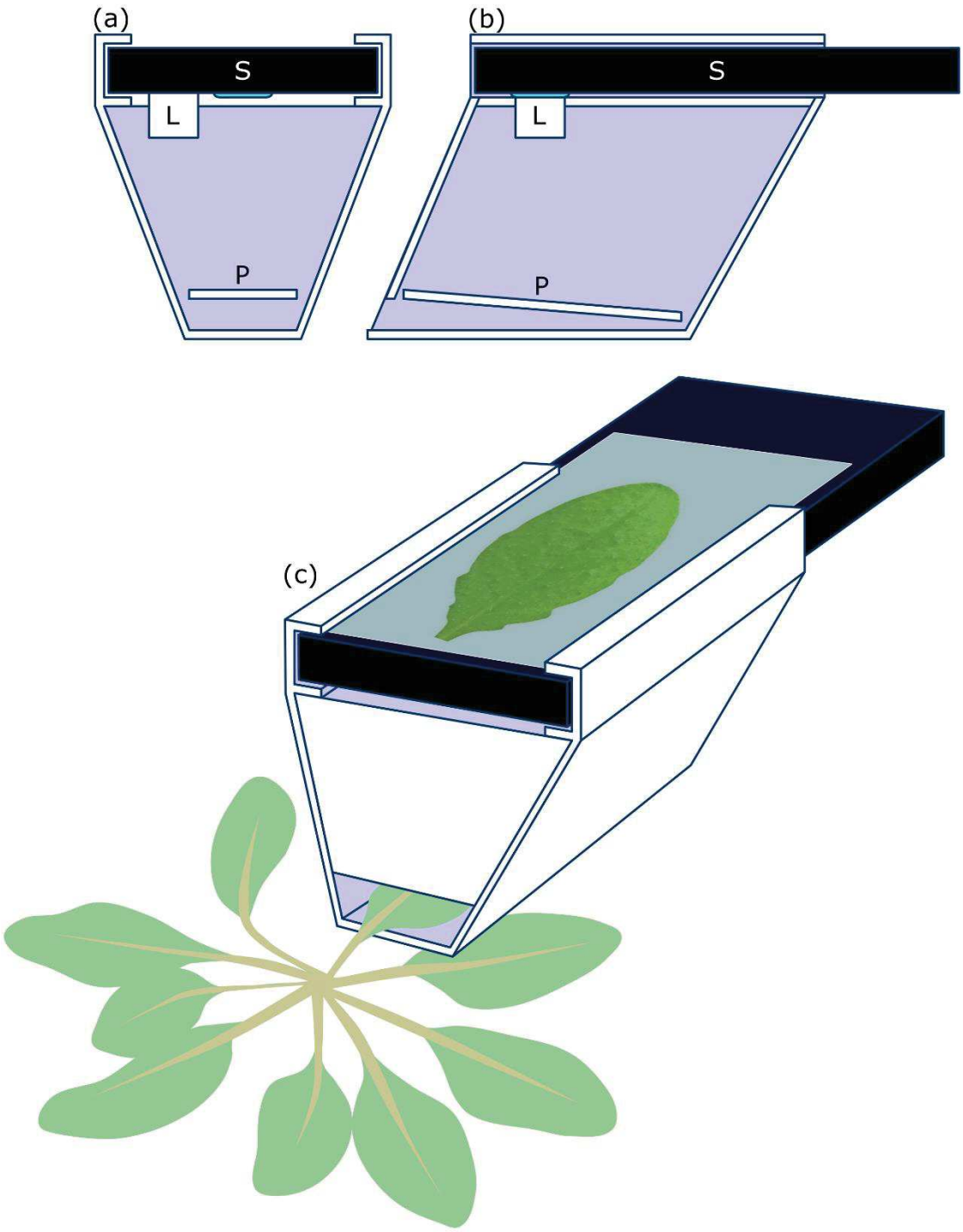

Figure S1: Diagram of the device used for measuring leaf area without cutting the leaf. (a) Frontal section, (b) sagittal section, and (c) three-dimensional view of the device. Abbreviations: (S) Smartphone, (L) light diffuser, (P) transparent piece of plastic.

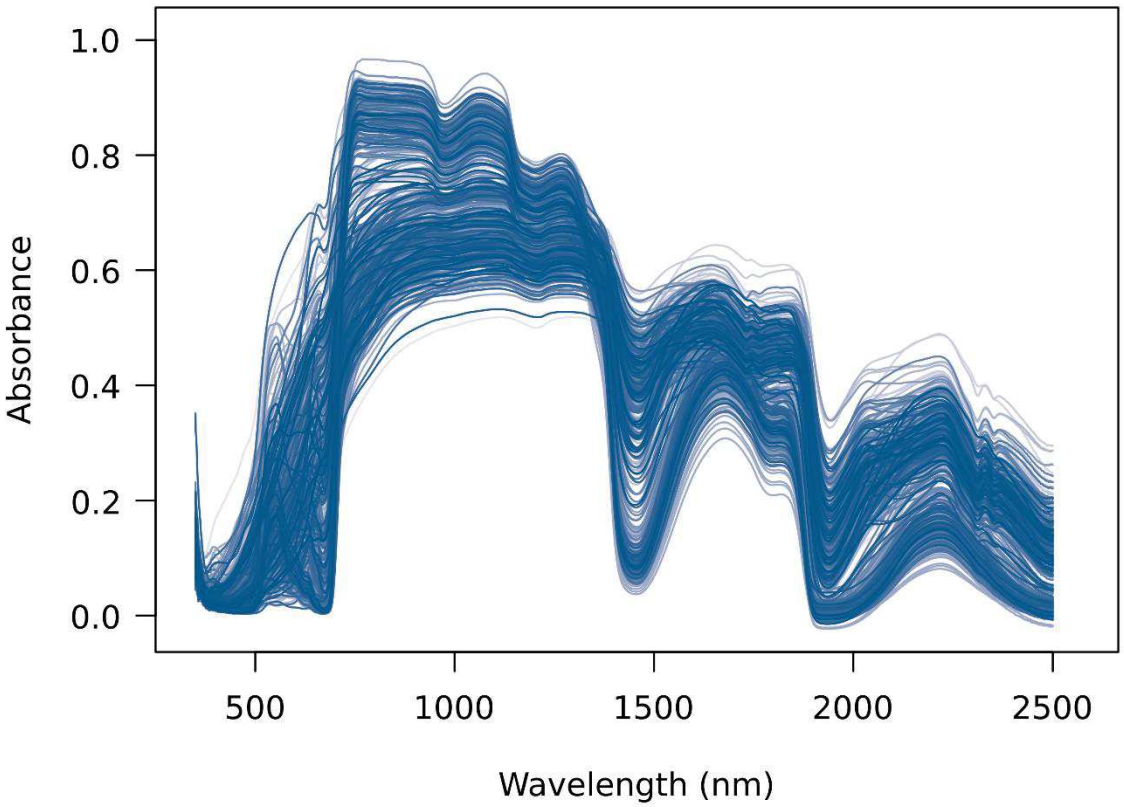

Figure S2: Absorbance spectra of fresh green to senescent leaves. Each blue line represents the averaged spectra acquired from the tip and edge of one leaf from one *A. thaliana* ecotype.

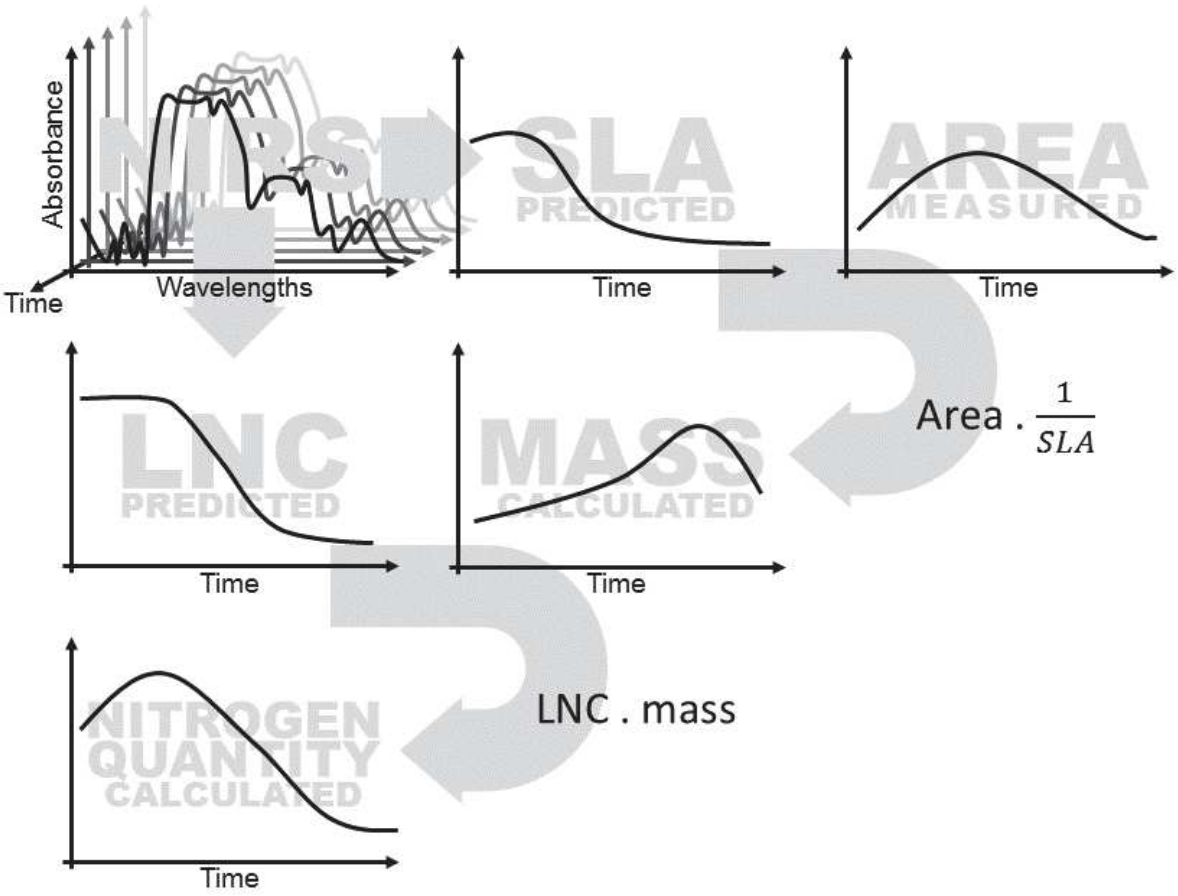

Figure S3. Procedure used to assess the dynamics of leaf nitrogen quantity. Leaf near infrared light absorbance (NIRS) was recorded through leaf aging to estimate the specific leaf area (SLA) and leaf nitrogen concentration (LNC). Leaf area was recorded daily. Combined estimates of SLA, LNC, and area, were used to calculate the dynamics of leaf dry mass (Mass) and leaf nitrogen quantity.

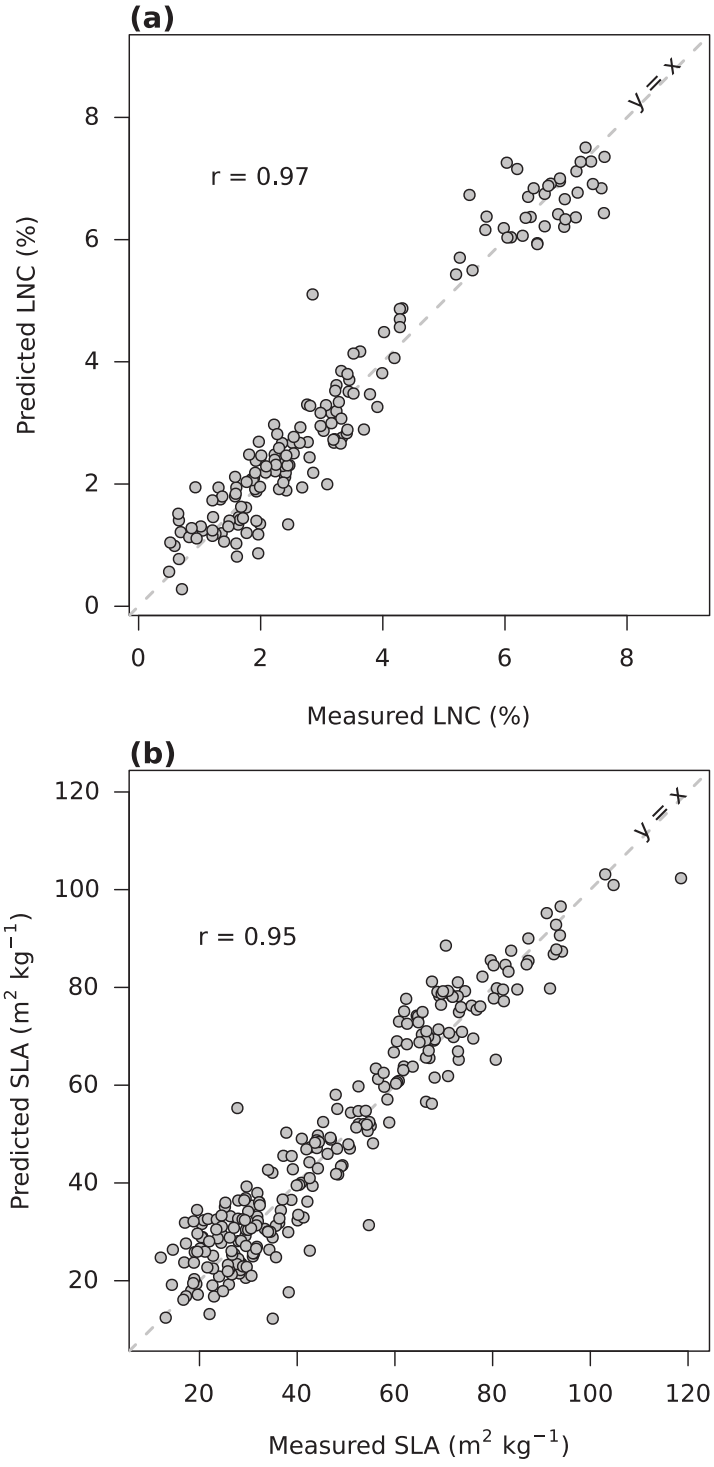

Figure S4. Performance of the predictive models for (a) leaf nitrogen concentration (LNC) and (b) specific leaf area (SLA).

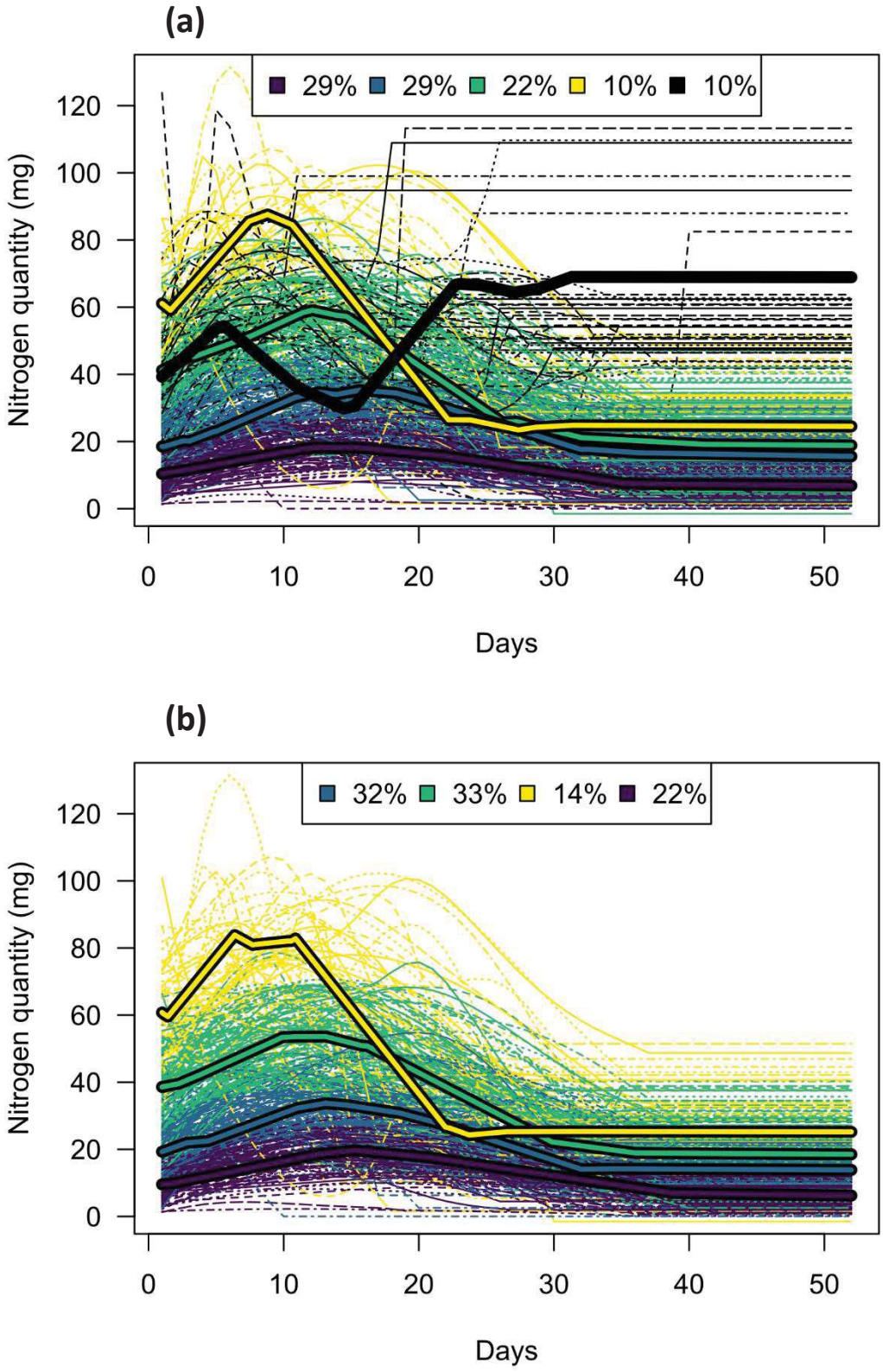

Figure S5. Result of the first step of klmShape clustering. (a) Initial clustering for the full dataset. Bold lines represent the average behavior of five different groups of nitrogen temporal variation. Dotted lines represent individual curves. Individuals from the fifth group (black line) were removed from the analysis and a second clustering were performed (b).

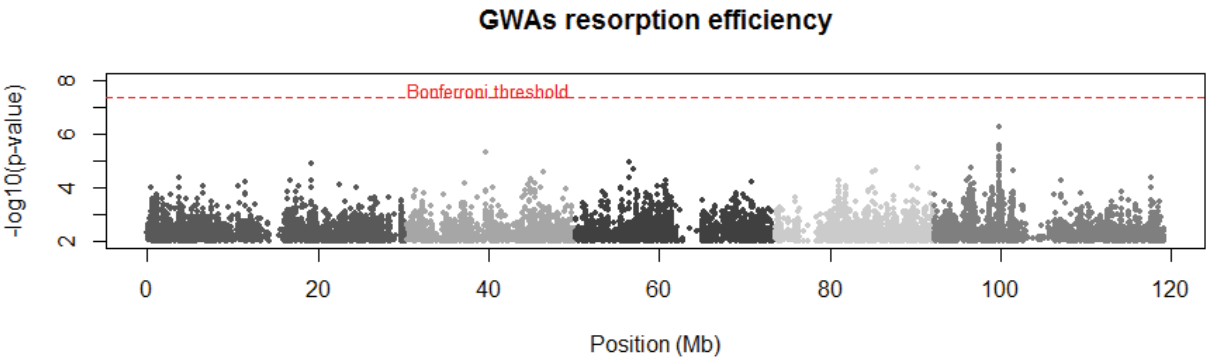

Figure S6. Genome-wide association study of the resorption efficiency. Each dot represents a single nucleotide polymorphism, its position along the x-axis reflects its position along the *Arabidopsis thaliana* genome, and its position along the y-axis gives the strength of the association. The red dashed line represents the significance threshold calculated with the Bonferroni method. Shades of grey delineate the five *A. thaliana* chromosomes.

Table S1: Accessions list. Abbreviations: FT, flowering time; BT, bolting time.

ID	FT	BT	name	CS number	country	latitude	longitude	group
10015	40,5	31,57	Ara-1	CS76382	AFG	37,29	71,3	asia
14313	56	48,5	Kos-2	CS78924	RUS	62,02	34,12	asia
159	52,75	42,17	MAR2-3	CS77070	FRA	47,35	3,93	western_europe
5151	66,75	62,4	UKSE06-325	CS78801	UK	52,2	-1,7	admixed
5165	56	48,14	UKSE06-362	CS78802	UK	51,3	0,4	admixed
5768	80,5	72,38	UKID63	CS78786	UK	54,1	-1,5	admixed
5784	67	57,14	Ty-1	CS78790	UK	56,4	-5,2	admixed
5837	45,5	34,5	Bor-1	CS76453	CZE	49,4	16,23	central_europe
6074	80,5	74,13	Or-1	CS77150	SWE	56,46	16,13	south_sweden
6076	87	84,2	Rev-2	CS77215	SWE	55,69	13,45	south_sweden
6108	54,5	44,25	T480	CS77300	SWE	55,8	13,12	western_europe
6151	73	66,5	T990	CS77328	SWE	55,65	13,22	south_sweden
6180	46,75	35,75	TaL 07	CS77339	SWE	62,63	17,69	germany
6184	67,67	58,8	TBO 01	CS77343	SWE	62,89	18,45	north_sweden
6195	58,33	49,29	TDr-9	CS77356	SWE	55,77	14,13	south_sweden
6209	67	54,29	TEDEN 02	CS77358	SWE	62,88	18,18	north_sweden
6243	44	35	Tottarp-2	CS77381	SWE	56,27	13,9	central_europe
6244	63	56,67	TRa 01	CS77384	SWE	62,92	18,47	north_sweden
6830	47,5	37,25	Kz-13	CS76994	KAZ	49,5	73,1	admixed
6897	47	38,13	Ag-0	CS76430	FRA	45	1,3	western_europe
6898	40,33	31,25	An-1	CS76435	BEL	51,22	4,4	admixed
6901	65,33	56,43	Bil-7	CS76710	SWE	63,32	18,48	north_sweden
6903	46,75	35,25	Bor-4	CS76454	CZE	49,4	16,23	central_europe
6904	48	38,75	Br-0	CS76455	CZE	49,2	16,62	western_europe
6909	47,5	39	Col-0	CS76778	USA	38,3	-92,3	germany
6911	35	24,75	Cvi-0	CS76789	CPV	15,11	-23,62	relict
6915	53,75	45,29	Ei-2	CS76478	GER	50,3	6,3	germany
6922	40,75	28,5	Gu-0	CS76498	GER	50,3	8	germany
6929	48	38,5	Kondara	CS76532	TJK	38,48	68,49	asia
6938	60	48,5	Ms-0	CS76555	RUS	55,75	37,63	asia
6945	57	49,5	Nok-3	CS76562	NED	52,24	4,45	germany
6958	41	29	Ra-0	CS76582	FRA	46	3,3	western_europe
6959	52,5	47	Rennes-1	CS77210	FRA	48,5	-1,41	western_europe
6963	69	59,38	Sorbo	CS78917	TJK	38,35	68,48	asia
6970	38,33	28,2	Ts-1	CS76615	ESP	41,72	2,93	spain
6979	35	25	Wei-0	CS76628	SUI	47,25	8,26	central_europe
6987	50,67	36,25	Ak-1	CS76431	GER	48,07	7,63	admixed
6989	47,5	38,63	Alst-1	CS76432	UK	54,8	-2,43	western_europe
7000	60	49,5	Aa-0	CS76428	GER	50,92	9,57	germany
7002	51,33	44,67	Baa-1	CS76442	NED	51,33	6,1	germany
7008	73,5	66,17	Benk-1	CS76447	NED	52	5,68	germany
7028	37,67	26,6	Bch-1	CS76444	GER	49,52	9,32	admixed
7063	50	36,63	Can-0	CS76740	ESP	29,21	-13,48	relict
7071	45,5	35,71	Chat-1	CS76463	FRA	48,07	1,34	western_europe

7077	35	24,25	Co-1	CS76468	POR	40,12	-8,25	italy_balkan_caucasus
7092	39	32	Com-1	CS76469	FRA	49,42	2,82	western_europe
7103	40,5	27,5	Dra-0	CS76476	CZE	49,42	16,27	central_europe
7111	49,25	37,75	Edi-0	CS76831	UK	55,95	-3,16	admixed
7127	45	34,6	Est	CS76485	EST	58,67	24,99	admixed
7143	49,67	37,4	Gel-1	CS76492	NED	51,02	5,87	germany
7165	52,5	40,63	Hn-0	CS76513	GER	51,35	8,29	germany
7186	45	34,25	Kn-0	CS76969	LTU	54,9	23,89	central_europe
7192	48	35,33	Kil-0	CS76526	UK	55,64	-5,66	germany
7209	45,25	34	La-0	CS76538	POL	52,73	15,23	admixed
7213	38,75	26	Ler-0	CS77020	GER	47,98	10,87	admixed
7287	52,5	40	Ove-0	CS76569	GER	53,34	8,42	germany
7288	70	60	Oy-0	CS77156	NOR	60,39	6,19	admixed
7298	56,5	45,57	Pi-0	CS76572	AUT	47,04	10,51	central_europe
7316	60,2	48,25	Rhen-1	CS78916	NED	51,97	5,57	admixed
7320	51	41	Rou-0	CS76591	FRA	49,44	1,1	western_europe
7347	43	34,5	Stw-0	CS76605	RUS	52	36	central_europe
7373	52	42,38	Tsu-0	CS77389	JPN	34,43	136,31	admixed
7382	37	27	Utrecht	CS76622	NED	52,09	5,11	admixed
7383	40,25	28,29	Van-0	CS76623	CAN	49,27	-123,21	western_europe
7394	39,67	27	Wa-1	CS76626	POL	52,3	21	admixed
7424	54	44	Jl-3	CS76519	CZE	49,2	16,62	central_europe
7461	44,25	32,14	H55	CS76897	CZE	49	15	germany
763	41	27,43	Kar-1	CS76522	KGZ	42,3	74,37	asia
8214	43,67	34,75	Gy-0	CS78901	FRA	49	2	western_europe
8231	92	79,67	Bro1-6	CS76726	SWE	56,3	16	south_sweden
8240	72,75	66,25	Kulturen-1	CS76987	SWE	55,71	13,2	south_sweden
8247	71	58,4	San-2	CS77233	SWE	56,07	13,74	south_sweden
8312	49	40	Is-0	CS78904	GER	50,5	7,5	germany
8343	46	41,63	Na-1	CS76558	FRA	47,5	1,5	admixed
8351	67,75	54,75	Ost-0	CS77154	SWE	60,25	18,37	north_sweden
8354	44,5	32,25	Per-1	CS76571	RUS	58	56,32	asia
8357	46	35,5	Pla-0	CS76573	ESP	41,5	2,25	spain
8376	69,33	57,43	Sanna-2	CS77234	SWE	62,69	18	north_sweden
8424	39,33	27	Kas-2	CS78905	IND	35	77	asia
88	40,67	30,33	CYR	CS76790	FRA	47,4	0,68	western_europe
9057	58,25	49,25	Vinslov	CS78847	SWE	56,1	13,92	south_sweden
9437	64,5	60,67	Puk-2	CS77195	SWE	56,16	14,68	south_sweden
9507	35	22	Coa-0	CS76775	POR	38,45	-7,5	spain
9518	66	60,17	Alm-0	CS76660	ESP	39,88	-0,36	spain
9524	61	47,5	Ber-0	CS78887	ESP	42,52	-0,56	spain
9535	54,5	37,29	Coc-1	CS76776	ESP	42,31	3,19	spain
9537	38,33	26,5	Cum-1	CS76787	ESP	38,07	-6,66	spain
9544	36,67	25,67	Gua-1	CS76894	ESP	39,4	-5,33	spain
9548	95	76	Hoy-0	CS76939	ESP	40,4	-5	admixed
9549	71,75	61,86	Hum-2	CS76943	ESP	42,23	-3,69	relict
9560	37	27,29	Mot-0	CS77109	ESP	38,19	-6,24	spain
9562	52	44,14	Mur-0	CS77115	ESP	41,67	2	spain
9567	82,67	72,2	Pal-0	CS77159	ESP	42,34	1,3	spain
9587	72,33	62,67	Tdc-0	CS77344	ESP	41,5	-1,88	spain

9589	66	62,6	Tor-1	CS77378	ESP	41,6	-2,83	spain
9594	78,5	69	Vdm-0	CS78837	ESP	42,04	1,01	spain
9598	65,25	54,86	Vim-0	CS78844	ESP	41,88	-6,51	relict
9606	36	25,86	Aitba-1	CS76649	MAR	31,48	-7,45	relict
9625	54	48,57	Kolyv-2	CS76977	RUS	51,31	82,59	asia
9637	50,25	40,14	Noveg-2	CS77132	RUS	51,77	80,85	asia
9640	71,5	62	Rakit-1	CS77202	RUS	51,87	80,06	asia
9649	53,5	46,4	Bivio-1	CS76713	ITA	39,13	16,17	italy_balkan_caucasus
9653	39,5	27,38	Giffo-1	CS76878	ITA	38,44	16,13	italy_balkan_caucasus
9657	35,5	25	Melic-1	CS77078	ITA	38,45	16,04	italy_balkan_caucasus
9697	53,25	40,75	Dolen-1	CS76802	BUL	41,62	23,94	italy_balkan_caucasus
9726	41	33,13	Faneronemi-3	CS76853	GRC	37,07	22,04	italy_balkan_caucasus
9737	56,75	48,75	Ulies-1	CS78815	ROU	45,95	22,62	asia
9738	50,25	43,13	Bran-1	CS76722	ROU	45,57	25,42	admixed
9741	52	46,75	Orast-1	CS77151	ROU	45,84	23,16	central_europe
9743	68	57,38	Furni-1	CS76873	ROU	45,14	25	admixed
9749	50	42,17	Knjas-1	CS76971	SRB	43,54	22,29	italy_balkan_caucasus
9758	47	38,5	Altai-5	CS76433	CHN	47,75	88,4	asia
9784	38,75	28	Erg2-6	CS76845	GER	48,5	8,8	central_europe
9927	40,25	27	ARR-17	CS76673	FRA	44,05	3,69	western_europe
9933	41,75	32	VED-10	CS78839	FRA	43,74	3,89	admixed
9941	52,67	40,33	Fei-0	CS76412	POR	40,92	-8,54	western_europe
9943	48,67	36	Cdm-0	CS76410	ESP	39,73	-5,74	spain
9944	51,33	42,83	Don-0	CS76411	ESP	36,83	-6,36	relict
9947	47	55,2	Ped-0	CS76415	ESP	40,74	-3,9	relict
9958	54,25	46,25	Shigu-1	CS76375	RUS	53,33	49,48	asia
9997	51,25	41,43	Rue3.1-31	CS76406	GER	48,56	9,16	central_europe

Table S2: Candidate gene list.

Name	Description	Position	Expressed in	Involved in
AT4G11060	Mitochondrially targeted single-stranded DNA binding protein	Chr4:6754515..6756595 (- strand)	Seed, growing tissues	Mitochondrial DNA replication, positive regulation of helicase activity
AT4G11070	WRKY family transcription factor	Chr4:6759098..6760794 (+ strand)	Senescent leaf (petiole/vein)	Regulation of transcription, DNA-templated
AT4G11080	HMG (high mobility group) box protein	Chr4:6760278..6763499 (- strand)	Inflorescences	Regulation of transcription, DNA-templated
AT4G05845	Long_noncoding_rna	Chr4:6763744..6763968 (+ strand)	Seed, growing tissues	
AT4G11090	TRICHOME BIREFRINGENCE-LIKE 23	Chr4:6764379..6766329 (- strand)	The whole plant	Synthesis and deposition of secondary wall cellulose
AT4G11100	Gelsolin protein	Chr4:6768614..6770285 (+ strand)	Inflorescences, young leaf	
AT4G11110	SPA1-related 2	Chr4:6771605..6777225 (+ strand)	Seed, flower, young leaf	Suppressing photomorphogenesis in dark- and light-grown seedlings